The Use of Nano-composite Ceramic Membranes for Gas Separations

Habiba Shehu, Edidiong Okon and Edward Gobina

Abstract— The preparation of composite ceramic inorganic membranes using different types of support with the aim to achieving high selectivity for lower hydrocarbons was studied. The pore size of the unmodified support was determined. Upon modification of the support, the morphology was examined using Scanning Electron Microscopy (SEM), which showed a reduction in the pore radius and pore size distribution. Gas permeation tests were carried out with inorganic ceramic membrane consisting of a ceramic support and a zeolite layer. The permeance of nitrogen, carbon dioxide, helium, methane, propane and argon through the membrane at varying pressures was determined. The effect of the mean pressure of up to 0.1 MPa on the molar flux of the gases at 294K was determined.

Index Terms— Composite membranes, Knudsen flow, permeance and selectivity.

I. INTRODUCTION

Gaseous hydrocarbons that are prevalent under increased pressure are solution gases in oil reservoirs. At equilibrium, they are in solution with the liquid hydrocarbon phase. These hydrocarbon gases are usually conserved but in some cases their storage is considered uneconomical and the gases are flared which is not an ideal practice. The impact of gas flaring cannot be over emphasized, it can cause detrimental effects to the environment [1], and these effects are highlighted below:

A. Emissions of methane and carbon dioxide: The main gases responsible for global warming are carbon dioxide and methane with methane being about 35 times more potent than carbon dioxide.

The reduction of the volume of gases wasted by flaring without compromising oil production can be achieved by exploiting gas conservation opportunities [2].

B. Nitrous oxide emissions in the presence of volatile organic compounds: The emissions of nitrous oxides in the presence of volatile organic compounds can lead to the formation of ground level ozone which can have a toxic effect to the vegetation and humans as well. Nitrogen oxide is a major contributor to acid rain as well.

C. Sulfur dioxide and hydrogen sulphide emissions: Hydrogen sulfide is a corrosive toxic gas that can be oxidized rapidly to sulfur dioxide, which is a contributor to acid rain. Many efforts have been made in the last couple of years to develop an effective method for the separation and subsequent removal of impurities from natural gas.

There are ongoing researches on the use of nano-composite membranes to separate gaseous mixtures hence making it one of the emerging technologies that is growing fast.

Its use has grown considerably both academically as well as industrially and they can be used for several applications. They are generally more fragile and expensive to fabricate than polymeric membranes but they can withstand more rigorous separation conditions that include high temperatures or corrosive solvents [3]. Ceramic membranes do not only have higher thermal and chemical stability but also have higher permeability as well [4]. There are several types of support used for these membranes. The supports used include zeolites, silica, alumina and stainless steel [5]. The various use of ceramic membranes include hydrogen separation and purification to get ultra-pure hydrogen, recovery of CO_2 from natural gas and power station flue gases and oxygen or nitrogen enrichment of air [6,7]. Ceramic membranes can also be incorporated into chemical reactors and thus serve as a catalyst by shifting the reaction equilibrium to the product [5].

Ceramic membranes that are available commercially generally have a pore size of 5 nm or bigger [8]. With the modification of these ceramic membranes the pore size may be reduced to near molecular dimensions, which enable separation of components based on the differences in adsorption or in the shape of the components [9]. There are various methods that can be used for the modification of membranes including deposition that aims at modification of an existing membrane by the formation of porous or non-porous layer on the membrane surface. Further processing by the means of annealing, carbonization or plasma treatment can follow the deposition for further optimization. Examples of deposition include: chemical vapor deposition (CVD), sol-gel deposition, Langmuir-Blodgett (LB) deposition, spins coating and self-assembly [3].

Transport properties of ceramic membranes can be explained as the movement of components through the membrane. There are various mechanisms that govern these transport properties. The differences in molecular weights of the components to be separated gives rise to Knudsen diffusion, which proceeds at a speed inversely proportional to the square root of the molecular weight of the component. However, separation by Knudsen diffusion requires that the pore diameter of the membrane to be smaller than the mean free path of the components. Generally, diffusion of gases through porous membranes is dependent on the type of collisions occurring. At low concentrations, where there is

predominantly molecule - pore wall collisions then the flow is Knudsen flow. At high concentrations where collisions are predominantly molecule – molecule then the flow is viscous flow. Knudsen flow can be achieved with membranes whose pore size is greater than 4 nm and the separation factor for a mixture of binary gases can be estimated from the square root of the ratio of the molecular weights of the gases also gas permeation by Knudsen diffusion varies inversely with the square root of the molecular weights of the gases. Hence an ideal separation for a mixture of binary gases is equal to the inverse of the square root of their molecular mass ratio [10]. The transportation equation for Knudsen and viscous flow is given by:

$$J = A\bar{P} + B \tag{1}$$

Where $\bar{P}$ is the average pressure across a porous membrane, A and B are constants relative to the membrane structure, molecular weight and size. According to equation (1), A is the constant representing viscous flow while B is the constant representing non-viscous flow, J is the permeability of the membrane and it is calculated using the equation:

$$J = \frac{Q}{S}.\bar{P} \tag{2}$$

Where Q is the flow rate in mols^{-1}, S is the membrane area. The pore radius of the membrane can be determined using the formula [11]:

$$rp = \frac{16.A.\mu}{3.B} \sqrt{8RT}/\pi M \tag{3}$$

Where M is the molar mass of the gas (g/mol), R is the molar gas constant (8.314 mol^{-1}J K^{-1}), T is the temperature in (K) and μ is the viscosity (Pa s^{-1}) of the gas.

The Knudsen number is given by:

$$K = \frac{D}{\lambda} \tag{4}$$

Where D is the pore diameter (m) and λ is the mean free path of the molecules (m) determines the flow regime of the membrane. When the diameter of the pores is lower than the mean free path of the molecules then Knudsen flow is dominant [11]. The assumptions made using this model is that there is negligible pressure drop due to the relatively small length of the capillaries used in this work [12].

Gas transport through α-Al$_2$O$_3$ support can involve both Knudsen and viscous flow when the interaction between the gas and the pore walls of a porous membrane is negligible [13].

Another way to explain transport mechanism in membranes is that when the membranes have pore diameters that are in between the sizes of the gas molecules to be separated in this case the membrane acts as a molecular sieve. These membranes are porous and there pore sizes are usually about 0.5 nm or bigger. If the gases to be separated have different atomic diameters then the smaller molecules will permeate through the membrane while the larger molecules will be retained, here very high selectivity could be achieved [10]. Surface diffusion is a transport mechanism where the diffusing species absorbs on the walls of the membrane pore and then rapidly moves across the surface to be permeated on the other side. Capillary condensation occurs when a porous membrane is in contact with a vapor; the saturation vapor pressure in the pores is different from the saturation vapor pressure of the components [14].

The contributions of the different transport mechanisms rely on the gases to be separated, the properties of the membrane as well as the operating conditions like temperature and pressure. For a commercial ceramic membrane, at elevated temperatures and low pressures the most likely transport mechanism employed is the Knudsen flow. Molecular sieving does not take place due to pore sizes being larger than the gas molecules [10]. The transport of gases through only Knudsen diffusion has been found to be inhibitive on the selectivity of a separating system. To overcome this difficulty, various efforts to promote other modes of transport have been made by surface modification [6].

This work looks at the transport mechanism exhibited by single gases through a ceramic porous membrane with an active silica layer.

II. Experimental

The schematic diagram of a membrane reactor used for the permeation test for the gases is given in Fig. 1. Four different gases: carbon dioxide, helium, nitrogen and argon were used to test for their permeability through a porous ceramic membrane at various pressures.
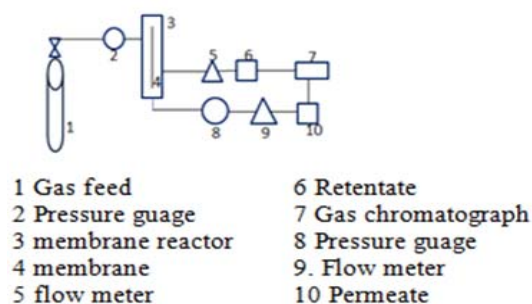

1 Gas feed	6 Retentate
2 Pressure guage	7 Gas chromatograph
3 membrane reactor	8 Pressure guage
4 membrane	9. Flow meter
5 flow meter	10 Permeate

Fig 1: Schematic diagram of a membrane reactor

A. Modeling of the silica membrane

Gas permeation test was carried out using the experimental rig depicted in Fig. 1, dip coating method was used to modify the membrane. The support layer comprises of a porous alumina which is dipped into a solution that comprises of Silicone elastomer, curing agent and isopentane in the ratio 10:1:100 respectively. The mixture was first homogenized with magnetic stirring for 2 hours before the support is dipped for 1 hour with constant stirring to prevent the mixture from gelatinizing. The membrane was air dried for 30 minutes and thermally treated at 333 K for 2 hours prior to permeation test. The membrane set up is shown in Fig. 2. The composition of the solution used for membrane modification is given in Table 1.

Table I: Composition of the modification solution

Silicone elastomer	50 ml
Curing agent	5 ml
Isopentane	500 ml

B. Modeling of the zeolite membrane

A solution containing Silicone oxide, aluminium oxide, sodium oxide and deionized water was prepared and homogenised at room temperature for 20 hours, the amount of each substance used is given in Table II. Zeolite crystals were deposited on alumina support that is subsequently dipped into the solution and kept for 20 hours at 343 K. The membrane was washed with deionized water and the pH of the rinse water was monitored. When the rinse water pH was neutral the membrane was air dried for 20 minutes and thermally treated in the oven at 338 K for 2 hours prior to permeation test.

Table II: Composition of the modification solution for zeolite membrane

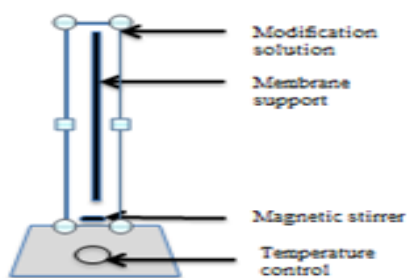| Chemical	Amount (ml)
Aluminium oxide	10
Sodium hydroxide	14
Deionised water	798
Silicone oxide	1

Fig 2: Membrane modification

C. Membrane Characterization

The morphology of the membrane was determined by the use of the scanning electron Microscope (SEM) and the elemental composition of the membrane was confirmed using Energy Dispersive X-Ray Analysis (EDAX).

III. RESULTS AND DISCUSSION

A. Gas permeation of silica membrane:

Fig. 3 shows the plot of permeance of the gases against the pressure drop across the membrane. The α–Al_2O_3 support showed permeance in the range of 10^{-5} $molm^{-2}Pa^{-1}$ for CO_2, Ar, N_2 and He at room temperature

The permeance decreased with increase in feed pressure, CO_2 has the lowest permeance but the highest molecular weight and He has the lowest molecular weight but highest permeance, hence this follows an inverse relationship between molecular weight and permeance which follows the flow mechanism of Knudsen flow[10]. At pressures higher than 0.1 bar the graph indicates a flow that is consistence with Knudsen flow for a membrane that is free from defects.

The order of molecular weights is CO_2 > Ar > N_2 > He nitrogen and argon have close permeance as can be observed in Fig. 3 but their molecular weights are not close. This could imply that a different flow mechanism was responsible for the transport of these gases across the membrane.
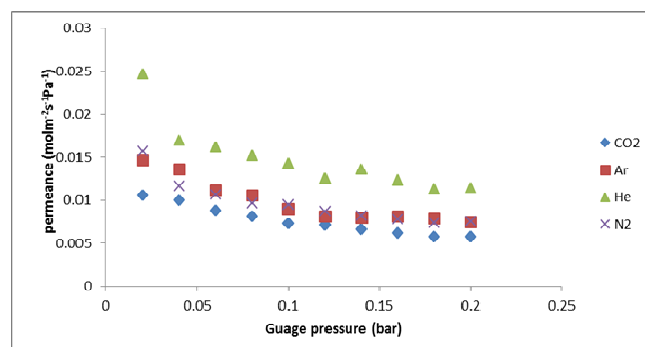

Fig 3: Effect of pressure on gas permeance of silica membrane at 298 K.

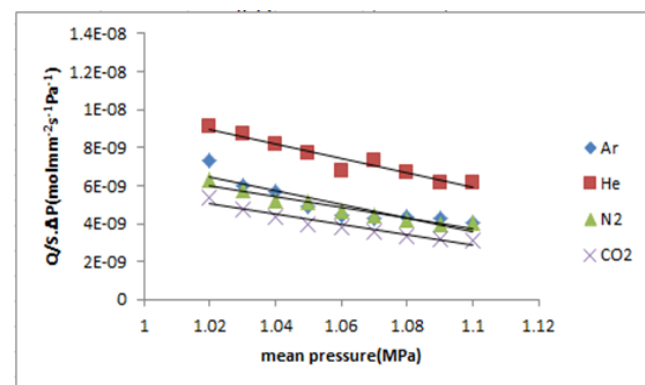Fig. 4 shows the plot of the permeability against the mean pressure.

Fig 4: Effect of mean pressure on the permeability of the gases

From the straight line equation;
$$y = mx + c$$
The slope (m) of the graph is the viscous contribution, while the intercept (c) is the contribution due non-viscous flow. From the graph the pore radius and the mean free path of the molecules was calculated and represented in Table II below.

Table II: Pore radius of the membrane and mean free path of the gases

	$r_p(m)$	$\lambda(m)$
Ar	0.037×10^{-10}	1.48×10^{-4}
He	0.312×10^{-10}	6.24×10^{-4}
N_2	0.044×10^{-10}	2.93×10^{-4}
CO_2	0.029×10^{-10}	1.99×10^{-4}

Theoretically the pore radius of the membrane is supposed to be the same. From Table II, it can be seen that the pore radius is much lower than the mean free path, which implies that the dominant flow of the gases is Knudsen flow.
The Knudsen selectivity was calculated using the ratios of the molecular weights of the gases[10] and is compared with the calculated permselectivity of the gases through the membrane (Fig. 5)
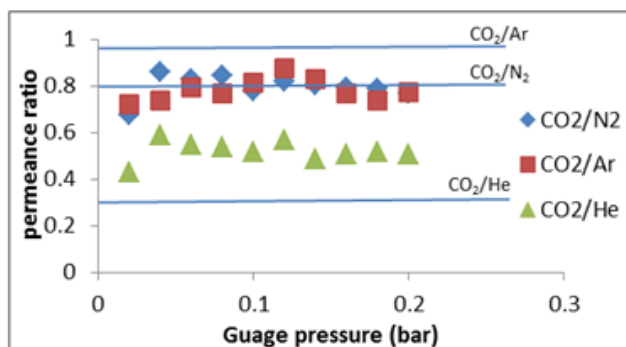
Fig 5: permselectivity with CO2 at room temperature.

The values of the Knudsen selectivity calculated for the gases are shown in Table III.

Table III: Knudsen selectivity calculated using the molecular weights of the gases

Gases	Knudsen selectivity
CO_2/N_2	0.799
CO_2/Ar	0.952
CO_2/He	0.302

The Knudsen selectivity calculated has shown higher values for CO_2/Ar at all the pressures used than the experimental Knudsen selectivity calculated using the ratio of the gas permeability. This could indicate another flow mechanism should be employed for the separation of these gases. For CO_2/He, the Knudsen selectivity calculated is lower than the experimental value that could indicate a good separation.

A plot of the permeance against the inverse of the square root of the molecular weights of the gases is given in Fig. 6.
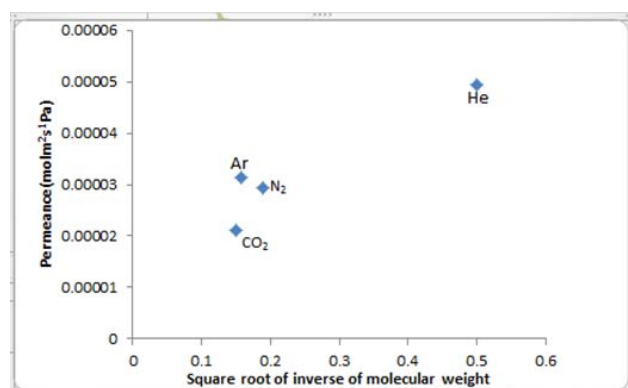

Fig 6: Permeance against inverse of the square root of the molecular weights of the gases.

The graph is not linear as expected for Knudsen flow mechanism.

To further explain the flow mechanism that the membrane exhibited, Fig. 7 is a plot of gas permeance at room temperature against the kinetic diameter of the gas molecules to see if the mechanism could be molecular sieving. According to Pandey and Chauhan[10] the smaller molecules will permeate while the larger molecules will be retained.
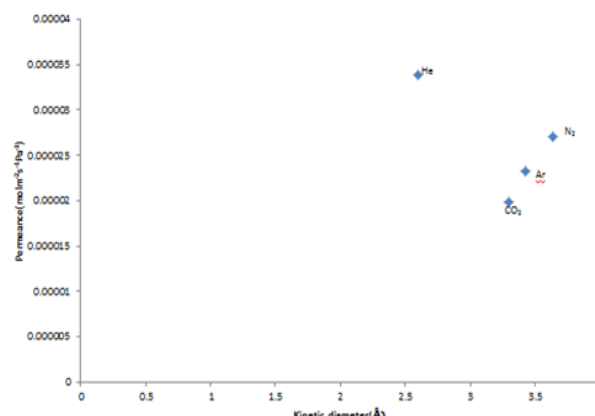

Fig 7: Permeance at 298 K and 2 kPa against kinetic diameter

The order of the kinetic diameter of the gases starting from the largest is $N_2 > Ar > CO_2 > He$. It can be seen that nitrogen having the highest kinetic diameter is permeating at a rate that is higher than argon and carbon dioxide which both have lower kinetic diameters. Fig. 8 proves that the membrane did not exhibit molecular sieving flow mechanism.

Nitrogen and argon have similar permeance although having different molecular weights. This could indicate there is a different flow mechanism that is responsible for the flow of these gases. The flux of nitrogen was determined and it showed an increase in flux with the increase in temperature.
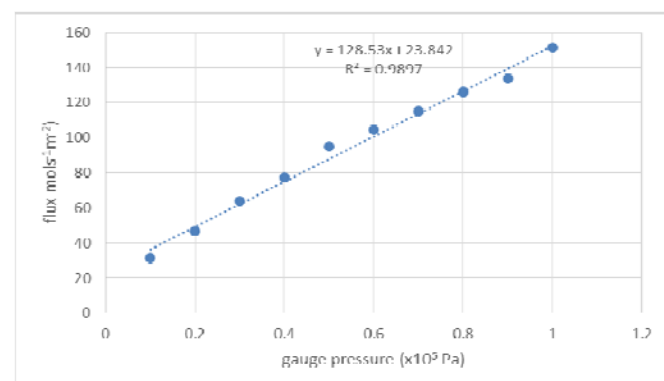

Fig 8: Effect of gauge pressure on the flux of nitrogen at 298 K using silica layer.

The flux of nitrogen as depicted in Fig. 8 increases linearly with increase in pressure, and it has a good correlation coefficient of 0.9897. The other gases (carbon dioxide, argon and helium) also had high fluxes at higher pressures.

B. Gas permeation of Y-type zeolite membrane:

The flux of propane, nitrogen and methane was determined through the zeolite layer. Fig. 9 depicts the flux of nitrogen and the permeances of propane, nitrogen and methane is depicted in Fig. 11.
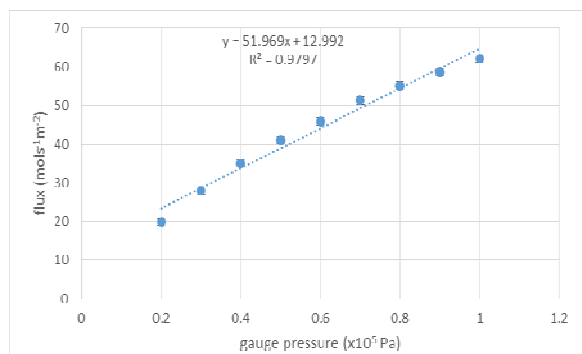
Fig 9: Effect of gauge pressure on the flux of nitrogen at 298 K using zeolite layer.
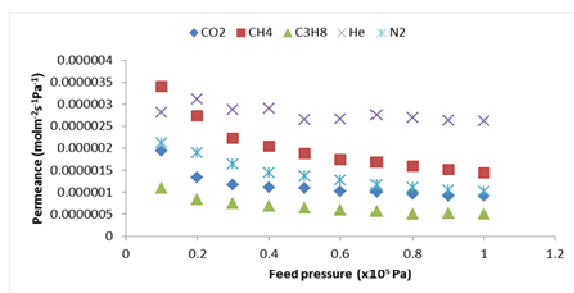

Fig 10: Effect of pressure on gas permeance of zeolite membrane at 298 K.

C. Membrane Characterization

The SEM images were collected in order to have an insight on the morphology of the selective layer. The cross section of the $\alpha–Al_2O_3$ ceramic membrane support is shown in Fig. 11 and the surface of the synthesized membranes is shown Fig. 12.

The pore size of the membrane can be estimated as 6 ± 0.2 μm. The thickness of the aluminium support can be estimate as 65 ± 0.2 μm.
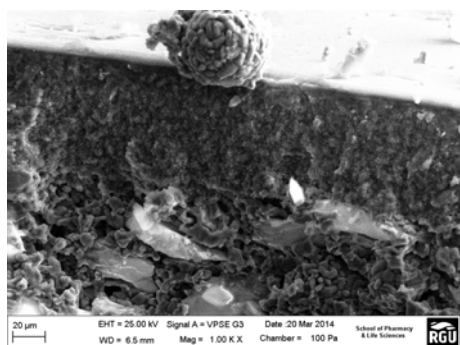

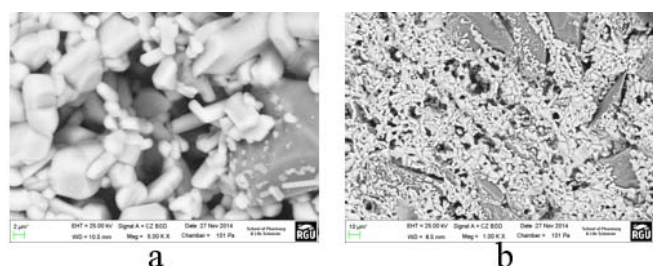Fig 11: Cross section image of $\alpha–Al_2O_3$ membrane support.

Fig. 12: The outer surface of (a) silica and (b) zeolite membrane.

The images in Figure 12 show the pore structure of the silica that is deposited on the aluminium support. Both the silica and zeolite are deposited on the support unevenly which could suggest that the pore size distribution could be unequal at different points of the membrane.

IV. SUMMARY AND CONCLUSIONS

To investigate gas separations efficiency of inorganic membranes, the support was modified and the flow mechanism employed by the membrane was determined. On the basis of the results obtained it can be concluded that the main mechanism governing the flow of gases through the modified silica membrane was Knudsen flow although there is evidence that another flow mechanism come to play. Further work should be carried out to determine how to modify a membrane support to get a specific flow mechanism. Studies from literature and preliminary experimental work have shown that for the separation of lower hydrocarbons, zeolite membranes have more efficacy than the silica or alumina ones. From the SEM images observed there is a need to modify the deposition of substances on a membrane support to achieve a defect free membrane with an even pore size distribution through the whole effective length of the membrane

REFERENCES

[1] Abedini R, Nezhadmoghadam A. Application of Membrane in Gas Separation Processes: Its Suitability and Mechanisms. *Petroleum & Coal.* 2010; 52(2):69-80.
[2] Tarmoon I. Middle East Oil Show. 1999
[3] Schüth F, Sing KSW, Weitkamp J. *Handbook of porous solids.* : Wiley-Vch; 2002.
[4] Huang P, Xu N, Shi J, Lin Y. Recovery of volatile organic solvent compounds from air by ceramic membranes. *Industrial & Engineering Chemistry Research.* 1997; 36(9):3815-3820.
[5] Li H, Schygulla U, Hoffmann J, Niehoff P, Haas-Santo K, Dittmeyer R. Experimental and modeling study of gas transport through composite ceramic membranes. *Chemical Engineering Science.* 2013;
.
[6] Baker RW. *Membrane technology.* : Wiley Online Library; 2000.
[7] Powell CE, Qiao GG. Polymeric CO< sub> 2</sub>/N< sub> 2</sub> gas separation membranes for the capture of carbon dioxide from power plant flue gases. *Journal of Membrane Science.* 2006; 279(1):1-49.
[8] Singh RP, Way JD, McCarley KC. Development of a model surface flow membrane by modification of porous vycor glass with a fluorosilane. *Industrial & Engineering Chemistry Research.* 2004; 43(12):3033-3040.
[9] van de Graaf, Jolinde M, Kapteijn F, Moulijn JA. Modeling permeation of binary mixtures through zeolite membranes. *AIChE Journal.* 1999; 45(3):497-511.
[10] Pandey P, Chauhan R. Membranes for gas separation. *Progress in Polymer Science.* 2001; 26(6):853-893.
[11] Julian A, Juste E, Chartier T, Del Gallo P and Richet N. Catalytic Membrane Reactor: Multilayer membranes elaboration. Catalytic Membrane Reactor: Multilayer membranes elaboration. *Proceedings of the 10th International Conference of the European Ceramic Society;* 2007. p. 718-722.
[12] Gobina EN, Oklany JS, Hughes R. Elimination of ammonia from coal gasification streams by using a catalytic membrane reactor. *Industrial & Engineering Chemistry Research.* 1995; 34(11):3777-3783.
[13] Li A, Zhao H, Gu J, Xiong G. Preparation of γ-A12O3 composite membrane and examination of membrane defects. *Science in China Series B: Chemistry.* 1997; 40(1):31-36.
[14] Sidhu PS, Cussler E. Diffusion and capillary flow in track-etched membranes. *Journal of Membrane Science.* 2001; 182(1):91-101